

Article

Superficial Velocity in Heterogeneous Two-Phase Systems with Truncated Fractal Distribution of Particle Concentration

Jianting Zhu 

Department of Civil and Architectural Engineering and Construction Management, University of Wyoming, Laramie, WY 82071, USA; jzhu5@uwyo.edu; Tel.: +1-307-766-4375

Abstract: The interplay of particles in a heterogeneous multiparticle two-phase system and its effect on superficial velocity have not been well quantified. In this study, a new model is developed to examine the superficial velocity in a heterogeneous multiparticle two-phase system. To examine the heterogeneous effects to the potentially maximum extent, the particle concentration is assumed to follow a truncated fractal distribution, which is integrated into the free surface cell model. In a statistical sense, the multiparticle two-phase system is stationary, so the mean of spatial heterogeneity can be replaced by the ensemble mean. Since the underlying physical concept is rooted in the free surface cell model, the validity of the model should be, therefore, limited to the low-Reynolds number conditions. The developed model is compared to data from three representative experimental studies in the literature and it is found that the model can better capture the scatters in experimental data than the original free surface cell model. The model is also compared with three representative models and demonstrates reasonable results. While the deterministic free surface cell model underestimates the velocity, the cell model with truncated fractal distribution being incorporated can predict high velocity with a wide range of particle concentration heterogeneity.

Keywords: heterogeneous multiparticle system; truncated fractal distribution; superficial velocity; free surface cell model



Citation: Zhu, J. Superficial Velocity in Heterogeneous Two-Phase Systems with Truncated Fractal Distribution of Particle Concentration. *Fluids* **2022**, *7*, 347. <https://doi.org/10.3390/fluids7110347>

Academic Editor:
Mehrdad Massoudi

Received: 4 October 2022
Accepted: 6 November 2022
Published: 9 November 2022

Publisher's Note: MDPI stays neutral with regard to jurisdictional claims in published maps and institutional affiliations.



Copyright: © 2022 by the author. Licensee MDPI, Basel, Switzerland. This article is an open access article distributed under the terms and conditions of the Creative Commons Attribution (CC BY) license (<https://creativecommons.org/licenses/by/4.0/>).

1. Introduction

The relative velocity of particles to fluid in a two-phase system is an essential parameter in many applications. Two cases of steady-state motion when either the particles move but there is no average flow of fluid, or the particles remain relatively stationary while fluid flows are often of particular interest. The presence of adjacent particles creates hindered superficial velocity effects, in which flow around the neighboring particles causes a larger drag than for a single particle, leading to a reduced superficial velocity of particles [1,2].

Sedimentation and fluidization are two important areas where understanding the superficial velocity is essential. For sedimentation, the reduced settling velocity of particles in a fluid is a critical physical parameter [3]. Baas et al. [4] reviewed experimental data sets of sediment settling velocity in the literature and proposed new empirical equations for a wide range of particle size and density, liquid density, and viscosity. Their results showed that the hindered effects started to impact the settling behavior of sediment particles at particle concentrations of only a few per cent. The settling velocity of particles depends on the diameter, the particle and fluid densities, and fluid viscosity. It also depends on other factors such as particle size distribution [5–8], particle shape, and its distribution [9–12]. Hanratty and Bandukwala [13] observed that at low Reynolds numbers, although the multiparticle system had a relatively uniform appearance, the particles were continually coming together in small groupings and then dispersing. As the Reynolds number increased, there were mass movements of groups of particles. In either case, there was heterogeneity in the particle distribution in the multiparticle system.

The fluidization of the particles takes place when the drag force on the particles balances their buoyant weight. For fluidization, Sun and Zhu [14] reviewed flow regimes

and developed a set of four-quadrant flow regime maps in fluidization systems. In upward gas–solid fluidization systems, the formation of bubbles (gas aggregation) or clusters (particle aggregation) due to the hydrodynamic effects, could result in heterogeneous structures [15] although the particle clustering phenomenon was less observed in liquid–solid fluidized beds [8,16]. In low-velocity gas–solid fluidization regimes, the particle-rich dense phase of particles and nearly particle-free dilute phase of fluid bubbles or voids could coexist [17], which would also result in a heterogeneous void and particle distributions. Felice et al. [18] analyzed mixing effects that may lead to continuously changing particle concentration relationships in heterogeneous binary-solid particulate fluidization. Patwardhan and Tien [19] calculated the stratified distribution of mixtures of particles and voids in liquid fluidized beds.

A widely used model for flow in multiparticle systems is the free surface cell model proposed by Happel [20]. In this model, each particle that was assumed to be uniformly spaced in the multiparticle system was enveloped by a spherical fluid cell. The fluid cell was proposed to represent the interactions between the particles. The radius of the fluid cell was determined so that the void space in the cell is equal to the voidage of the system and the shear stress on the cell surface is zero. The cell model was shown to well predict the drag but underestimate the superficial velocity for most fluidization and sedimentation systems [20]. Jean and Fan [21] proposed a model that included two additional factors of particle alignment and the nonuniformity of the local flow field (or channeling) and found that incorporating the nonuniformity effect of local voidage as well as the particle alignment effect could more satisfactorily account for the fluidization or the sedimentation velocity.

In summary, the interplay of various factors in a heterogeneous multiparticle two-phase system and its effect on the superficial velocity has not been well quantified. Correction factors for particle sorting in the superficial velocity equations have been rare. Mirza and Richardson [6] proposed a modified superficial velocity equation, which allowed for considering the effect of particle interactions. Maude and Whitmore [22] proposed a simple empirical power-law type equation with the power being related to the Reynolds number to allow for differences in particle shape and particle size distribution.

Overall, the effect of particle size distribution, or sorting, on the superficial velocity is less clear than the effect of particle shape. In this study, a new mathematical model is developed to examine the superficial velocity in a heterogeneous multiparticle two-phase system. It should be noted, however, that the proposed new model does not intend to directly address the particle size distribution and its effect on the superficial velocity of the two-phase system. Rather, it addresses the distribution heterogeneity of the particle concentration of the two-phase systems. This type of heterogeneous distribution considers the fact that in a portion of the region, the particle concentration is higher than the other locations. To incorporate the heterogeneity to the potentially maximum extent, the particle concentration is assumed to follow a truncated fractal distribution, which is then incorporated into the free surface cell model [20] to account for particle concentration heterogeneity. In a statistical sense, the multiparticle two-phase system is assumed to be stationary so the mean of the spatial heterogeneity can be replaced by the ensemble mean. As the underlying physical foundation is rooted in the free surface cell model, the validity of the model is, therefore, limited to low-Reynolds number flow conditions as in the cell model. The developed model is compared to data sets from three representative experimental studies in the literature and is also compared with three representative models in the literature. The impact of the fractal distribution on the mean and standard deviation of the superficial velocity ratio on the heterogeneous multiparticle system over that of a single particle is then quantified and discussed.

2. Methods

In this study, the local superficial velocity ratio is represented by the free surface model [20], in which two concentric spheres are considered. The radius of the spherical solid particle inside the cell represents the average radius of the particles in the two-phase

system. The radius of the outer fluid envelope is determined by the constraint that the volume fraction of particles in the two-phase system must be the same as the particle volume fraction of the cell. The model is referred to as the free surface model since it is assumed that it is frictionless on the outer fluid cell surface (i.e., the shear stress is zero) so the mathematical statement is closed to assure a unique solution. The solution of velocity distribution can be solved, and the superficial velocity is determined to be related to the overall pressure gradient. The superficial velocity is then normalized by the velocity of a single particle under the same pressure gradient condition to obtain the superficial velocity ratio, which is expressed in Equation (1) below. Refer to [20,23,24] for more detail about the free surface cell model.

$$V_r = 1 - (3/2)c^{1/3} + \frac{(5/6)c^{5/3}}{1 + (2/3)c^{5/3}} \tag{1}$$

where V_r is the ratio of superficial velocity V over the velocity of a single particle V_0 . (i.e., $V_r = V/V_0$) and c is the particle concentration (i.e., the volume fraction of the particles) in the two-phase multiparticle system.

While the original free surface cell model conceptualizes the two-phase system as a single sphere being surrounded by a fluid cell uniformly, the cell model is extended to represent the potential heterogeneity of the particles in the system. Locally the system is similarly conceptualized by the free surface cell, but the particle concentration can vary spatially. The particle concentration of a two-phase system is assumed to follow the following fractal distribution [25,26]

$$N(C \geq c) = (c_{max}/c)^{D/3} \tag{2}$$

where c_{max} is the maximum particle concentration and is assumed to be 1 for simplicity. It can be, however, other values smaller than 1. D is the fractal dimension of the characteristic length of the particle volume such as the effective diameter. Note that for an exact fractal distribution, the minimum value of c should start from 0. In this study, we approximate the particle concentration as a truncated fractal distribution in which the concentration starts from $c = c_{min}$ for practical applications.

The number of cells in the heterogeneous multiparticle system that is in the range from c to $c + dc$ can then be determined

$$- dN(c) = (D/3)c_{max}^{D/3}c^{-(D+3)/3}dc \tag{3}$$

The total number of cells, N_t , can be established by integrating over the entire range of particle concentration from c_{min} to c_{max} as

$$N_t = - \int_{c_{min}}^{c_{max}} dN(c) = (c_{max}/c_{min})^{D/3} - 1 \tag{4}$$

The probability density function of the truncated fractal distribution is then

$$f(c) = - \frac{dN}{N_t dc} = \frac{Dc_{min}^{D/3}c^{-(D/3+1)}}{3[1 - (c_{max}/c_{min})^{-D/3}]} \tag{5}$$

The mean concentration c^* in the two-phase system can then be determined as

$$c^* = \int_{c_{min}}^{c_{max}} cf(c)dc = \frac{Dc_{max}[(c_{max}/c_{min})^{-D/3} - (c_{max}/c_{min})^{-1}]}{(3 - D)[1 - (c_{max}/c_{min})^{-D/3}]} \tag{6}$$

With the given values of c^*/c_{\max} and D , the ratio c_{\max}/c_{\min} can be determined from the following constraint iteratively

$$\frac{c^*}{c_{\max}} = \frac{D[(c_{\max}/c_{\min})^{-D/3} - (c_{\max}/c_{\min})^{-1}]}{(3 - D)[1 - (c_{\max}/c_{\min})^{-D/3}]} \tag{7}$$

The variance s_c^2 and standard deviation s_c of the particle concentration can be calculated as follows, respectively

$$s_c^2 = (c^2)^* - c^{*2} = \frac{Dc_{\min}^2[(c_{\max}/c_{\min})^{2-D/3} - 1]}{(6 - D)[1 - (c_{\max}/c_{\min})^{-D/3}]} - \frac{D^2c_{\min}^2[(c_{\max}/c_{\min})^{1-D/3} - 1]^2}{(3 - D)^2[1 - (c_{\max}/c_{\min})^{-D/3}]^2} \tag{8}$$

$$s_c = \left\{ \frac{Dc_{\min}^2[(c_{\max}/c_{\min})^{2-D/3} - 1]}{(6 - D)[1 - (c_{\max}/c_{\min})^{-D/3}]} - \frac{D^2c_{\min}^2[(c_{\max}/c_{\min})^{1-D/3} - 1]^2}{(3 - D)^2[1 - (c_{\max}/c_{\min})^{-D/3}]^2} \right\}^{1/2} \tag{9}$$

The mean superficial velocity ratio, V_r^* , is determined by the following integration

$$V_r^* = \int_{c_{\min}}^{c_{\max}} \left[1 - (3/2)c^{1/3} + \frac{(5/6)c^{5/3}}{1 + (2/3)c^{5/3}} \right] f(c)dc \tag{10}$$

After the integration of the first two terms, one can obtain

$$V_r^* = 1 - \frac{3Dc_{\min}^{1/3}[1 - (c_{\max}/c_{\min})^{(1-D)/3}]}{2(D - 1)[1 - (c_{\max}/c_{\min})^{-D/3}]} + \frac{5Dc_{\min}^{D/3} \int_{c_{\min}}^{c_{\max}} \frac{c^{(2-D)/3}}{1 + (2/3)c^{5/3}} dc}{18[1 - (c_{\max}/c_{\min})^{-D/3}]} \tag{11}$$

The integration term $\int_{c_{\min}}^{c_{\max}} \frac{c^{(2-D)/3}}{1 + \frac{2}{3}c^{5/3}} dc$ in the above equation can be carried out by a variable transformation $z = c^{5/3}$ as follows

$$\int_{c_{\min}}^{c_{\max}} \frac{c^{(2-D)/3}}{1 + (2/3)c^{5/3}} dc = \frac{3c_{\min}^{(5-D)/3}}{5 - D} [(c_{\max}/c_{\min})^{(5-D)/3} G_1 - G_2] \tag{12}$$

where G_1 , and G_2 are the hypergeometric functions as follows, respectively

$$G_1 = {}_2F_1\left(1, 1 - D/5; 2 - D/5; -2c_{\max}^{5/3}/3\right) \tag{13}$$

$$G_2 = {}_2F_1\left(1, 1 - D/5; 2 - D/5; -2c_{\min}^{5/3}/3\right) \tag{14}$$

Therefore, the mean superficial velocity ratio is

$$V_r^* = 1 - \frac{3Dc_{\min}^{1/3}[1 - (c_{\max}/c_{\min})^{-(D-1)/3}]}{2(D - 1)[1 - (c_{\max}/c_{\min})^{-D/3}]} + \frac{5Dc_{\min}^{5/3}[(c_{\max}/c_{\min})^{(5-D)/3} G_1 - G_2]}{6(5 - D)[1 - (c_{\max}/c_{\min})^{-D/3}]} \tag{15}$$

The variance of the superficial velocity ratio is then integrated as

$$s^2 = \frac{9}{4} \left[\frac{c^{2/3}}{c^{1/3}} - \left(\frac{c^{1/3}}{c^{1/3}} \right)^2 \right] - \frac{5}{2} \left[\frac{c^2}{1 + (2/3)c^{5/3}} - \left(\frac{c^{1/3}}{c^{1/3}} \right) \left(\frac{c^{5/3}}{1 + (2/3)c^{5/3}} \right) \right] + \frac{25}{36} \left[\frac{c^{10/3}}{(1 + (2/3)c^{5/3})^2} - \left(\frac{c^{5/3}}{1 + (2/3)c^{5/3}} \right)^2 \right] \tag{16}$$

where the overbar denotes an average operator. The terms in Equation (16) can be evaluated and listed as follows, respectively

$$\overline{c^{1/3}} = \begin{cases} \frac{Dc_{\min}^{1/3} [1 - (c_{\max}/c_{\min})^{-(D-1)/3}]}{(D-1) [1 - (c_{\max}/c_{\min})^{-D/3}]} & \text{if } D \neq 1 \\ \frac{c_{\min}^{1/3} \ln(c_{\max}/c_{\min})}{3 [1 - (c_{\max}/c_{\min})^{-1/3}]} & \text{if } D = 1 \end{cases} \quad (17)$$

$$\overline{c^{2/3}} = \begin{cases} \frac{Dc_{\min}^{2/3} [1 - (c_{\max}/c_{\min})^{-(D-2)/3}]}{(D-2) [1 - (c_{\max}/c_{\min})^{-D/3}]} & \text{if } D \neq 2 \\ \frac{2c_{\min}^{2/3} \ln(c_{\max}/c_{\min})}{3 [1 - (c_{\max}/c_{\min})^{-2/3}]} & \text{if } D = 2 \end{cases} \quad (18)$$

$$\frac{\overline{c^{5/3}}}{1 + (2/3)c^{5/3}} = \frac{Dc_{\min}^{5/3} [(c_{\max}/c_{\min})^{(5-D)/3} G_1 - G_2]}{(5 - D) [1 - (c_{\max}/c_{\min})^{-D/3}]} \quad (19)$$

$$\frac{\overline{c^2}}{1 + (2/3)c^{5/3}} = \frac{Dc_{\min}^2 [(c_{\max}/c_{\min})^{(6-D)/3} G_3 - G_4]}{(6 - D) [1 - (c_{\max}/c_{\min})^{-D/3}]} \quad (20)$$

where G_3 and G_4 are the hypergeometric functions as follows, respectively

$$G_3 = {}_2F_1 \left[1, (6 - D)/5; (11 - D)/5; -2c_{\max}^{5/3}/3 \right] \quad (21)$$

$$G_4 = {}_2F_1 \left[1, (6 - D)/5; (11 - D)/5; -2c_{\min}^{5/3}/3 \right] \quad (22)$$

$$\frac{\overline{c^{10/3}}}{(1 + \frac{2}{3}c^{5/3})^2} = \frac{Dc_{\min}^{10/3} [(c_{\max}/c_{\min})^{(10-D)/3} G_5 - G_6]}{(10 - D) [1 - (c_{\max}/c_{\min})^{-D/3}]} \quad (23)$$

The hypergeometric functions G_5 and G_6 in Equation (23) are, respectively

$$G_5 = {}_2F_1 \left(2, 2 - D/5; 3 - D/5; -2c_{\max}^{5/3}/3 \right) \quad (24)$$

$$G_6 = {}_2F_1 \left(2, 2 - D/5; 3 - D/5; -2c_{\min}^{5/3}/3 \right) \quad (25)$$

To summarize, there are two required input parameters of mean particle concentration c^* and fractal dimension D in the developed approach in this study. From the given c^* and D , we can first determine the ratio of maximum particle concentration c_{\max} (typical 1.0 or a smaller value) and minimum concentration c_{\min} , c_{\max}/c_{\min} from Equation (7) by iteration. After determining the c_{\max}/c_{\min} , we can calculate the variance and standard deviation of the particle concentration from Equations (8) and (9), respectively. The mean and standard deviation of the superficial velocity ratio are calculated from Equations (15) and (16), respectively. In the next section, we will compare the developed model to a few representative experimental data sets and models from the literature over the last six decades. The comparison with the experimental results is quantitatively assessed using the root mean square error (RMSE) and the Nash–Sutcliffe model efficiency coefficient (NSE). We will then discuss the impact of fractal dimension and the mean particle concentration on the superficial velocity ratio in more general perspectives.

3. Results

There have been numerous experimental data for both fluidization and sedimentation in the literature. In this section, the developed model is first compared to representative experimental data sets in the literature from three different studies conducted over the last six decades in 1957, 1992, and 2022, respectively, for both fluidization and sedimentation with various particle materials.

In Figure 1, the comparison of superficial velocity ratio is plotted with the experimental data from two typical runs for both the sedimentation and fluidization of Hanratty and Bandukwala [13]. The fluidization and sedimentation of 0.56 mm steel spheres and 0.71 mm glass spheres in glycerine-water solutions were studied experimentally in a 10.2 cm glass column. The experimental results of a typical run with a Reynolds number between 0.01 and 0.025 for both fluidization and sedimentation were used for comparison in this study. The model results of mean superficial velocity ratio based on the truncated fractal distribution are plotted in Figure 1 along with the mean \pm one standard deviation from the mean superficial velocity. The results from the simple deterministic uniform free surface cell model are also plotted for comparison. The truncated fractal distribution model results from both the small fractal dimension ($D = 1.1$) and the large fractal dimension ($D = 2.9$) are shown in Figure 1a,b, respectively. For the small fractal dimension, the structure of particle volume is less space filled with large dilute clusters (large void space). For the large fractal dimension close to 3, the particle volume is more space filled and tends to occupy spaces with small voids. Since both structures have the same mean particle concentration, the one with smaller fractal dimension should span a larger range of concentration range c_{\max}/c_{\min} so the particles can be in the dilute regions to make the overall mean concentration the same for both smaller fractal dimensions and larger fractal dimensions.

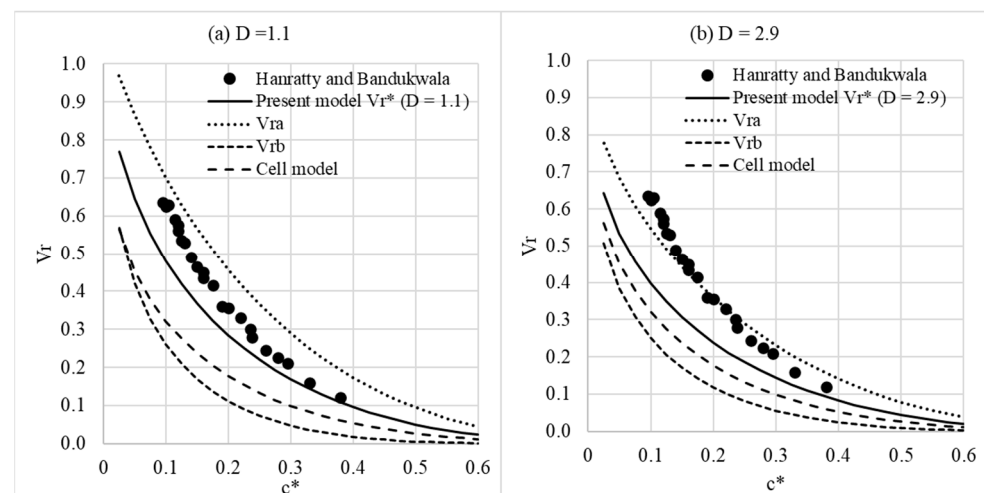


Figure 1. Comparison with early experimental data from typical runs of Hanratty and Bandukwala [13] for both the sedimentation and fluidization of steel spheres and glass spheres with (a) $D = 1.1$ and (b) $D = 2.9$. In (a,b), $V_{ra} = V_{r^*} + s$ and $V_{rb} = V_{r^*} - s$.

It can be seen that the two-phase system with the truncated fractal dimension predicts a higher mean concentration than the deterministic free surface cell model. Overall, however, the mean from the truncated fractal distribution still slightly underestimates the experimental data. The mean \pm standard deviation results can mostly capture the scatters in the experimental data, especially when the fractal dimension is small (Figure 1a). Since the interaction and hindered characteristics in affecting the superficial velocity ratio are highly non-linear and the velocity drops quickly with the increased particle concentration, the smaller fractal dimension system should have a higher chance of occupying the dilute regions that will enhance the superficial velocity compared to the large fractal dimension counterpart with the same mean particle concentration. Quantitatively for $D = 1.1$, the RMSE and NSE for the mean superficial velocity ratio prediction from this study are 0.099 and 0.598, respectively, while for $D = 2.9$, the RMSE and NSE are 0.155 and 0.004, respectively. For the deterministic free surface cell model prediction, the RMSE is higher at 0.219 and NES lower at -0.974 , respectively.

Figure 2 shows the comparison of the present model with the experimental results of Chianese et al. [10] for fluidization with irregularly shaped particles. Chianese et al. [10]

experimentally investigated the behavior of fluidized beds of monosized sodium perborate crystals in saturated aqueous solutions. The crystalline particles of 300 μm to 710 μm sieved in five size ranges were used in the experiments. More than 12 measurements were performed for each crystal set by gradually decreasing the flow rate of the fluidizing medium. The Reynolds number range was from 6.6 to 31 in the experiments of Chianese et al. [10]. For $D = 1.1$, the RMSE and NSE for the mean superficial velocity ratio prediction from this study are 0.024 and 0.940, respectively, while for $D = 2.9$, the RMSE and NSE are 0.036 and 0.860, respectively. For the deterministic free surface cell model prediction, the RMSE and NSE are 0.081 and 0.293, respectively.

Recently, Baas et al. [4] conducted five series of settling column experiments in which fresh water and well-sorted to very-well-sorted spherical glass beads with the mean size ranging from 0.040 mm to 0.552 mm were used. The superficial velocity was measured for particle concentration between 5% and 55%. The Reynolds number in the experiments by Baas et al. [4] ranged from 0.057 to 44.08. Figure 3 shows the comparison of the present study with recent experimental data from Baas et al. [4] for sedimentation of well-sorted spherical glass beads with $D = 1.1$ (Figure 3a) and $D = 2.9$ (Figure 3b). Under the very dilute conditions of particle concentration of a few volumetric percent, while the heterogeneously truncated fractal distribution of particle concentration enhances the superficial velocity significantly, it still slightly underpredicts the superficial velocity.

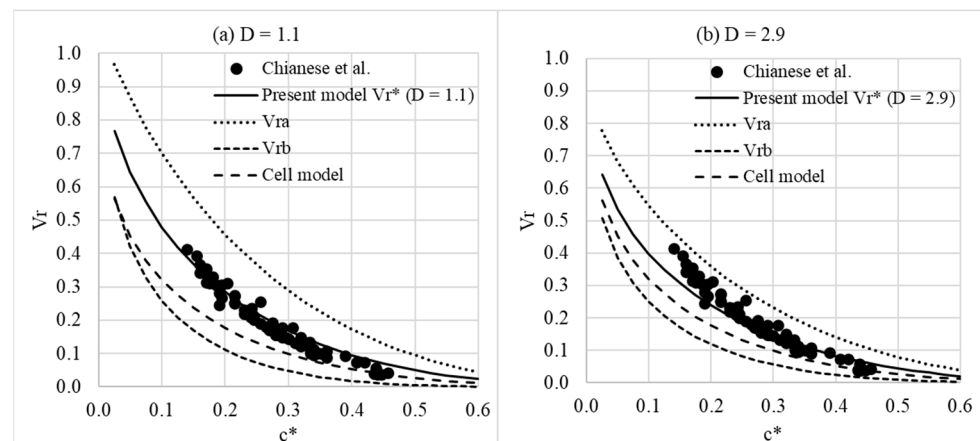


Figure 2. Comparison with experimental data from Chianese et al. [10] for the fluidization of irregular shape particles with (a) $D = 1.1$ and (b) $D = 2.9$. In (a,b), $V_{ra} = V_{r^*} + s$ and $V_{rb} = V_{r^*} - s$.

For $D = 1.1$, the RMSE and NSE for the mean superficial velocity prediction from this study are 0.078 and 0.905, respectively, while for $D = 2.9$ the RMSE and NSE are 0.112 and 0.806, respectively. For the deterministic free surface cell model prediction, the RMSE and NSE are 0.152 and 0.645, respectively. The smaller fractal dimension model prediction agrees better with the experimental data. Due to wide range of conditions, the experimental data exhibited large scatters, but the present model results follow the trend well. Overall, the mean \pm standard deviation band from the model prediction in this study is able to cover the scatters from the representative experimental results. The high value of the superficial velocity ratio in one set of experimental results by Baas et al. [4] at a high Reynolds number is slightly outside the mean \pm standard deviation envelope from the present study. The results from the experiments by Baas et al. [4] indicated that the superficial velocity ratio increased with the increasing Reynolds number. Therefore, the results that are under-predicted by the present study are for $Re = 44.08$, where the slow flow assumption presented in this study is likely to be deviated.

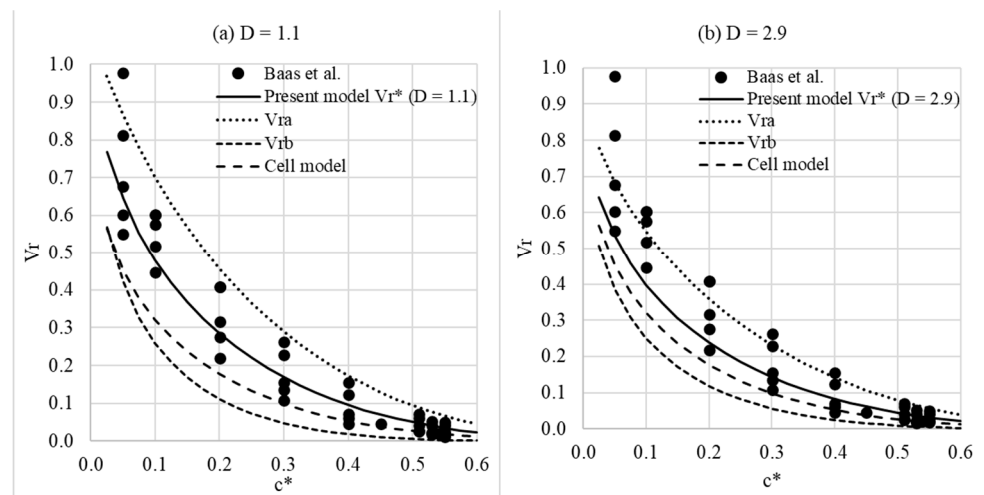


Figure 3. Comparison with recent experimental data from Baas et al. [4] for sedimentation of well-sorted spherical glass beads with (a) $D = 1.1$ and (b) $D = 2.9$. In (a,b), $V_{ra} = V_{r^*} + s$ and $V_{rb} = V_{r^*} - s$.

Figure 4 shows the results of the concentration c_{max}/c_{min} ratio in relation to the mean particle concentration (Figure 4a) and the fractal dimension (Figure 4b). The ratio c_{max}/c_{min} decreases quickly with the increase in the mean particle concentration. For dilute system with small particle concentration, the c_{min} needs to be small (i.e., high c_{max}/c_{min} ratio) for the system to achieve small mean particle concentrations given that c_{max} can only be as high as 1. Therefore, for a small fractal dimension, the contrast of particle concentration needs to be large as the system is less space-filled. As the mean particle concentration increases, the fractal distribution has to be more truncated, so it deviates from a truly fractal distribution more significantly since the distribution samples a smaller concentration range (i.e., c_{min} also increases). The contrast of c_{max}/c_{min} is, however, more pronounced under the small fractal dimension condition. In other words, the c_{min} should start at smaller value compared to a larger fractal dimension system.

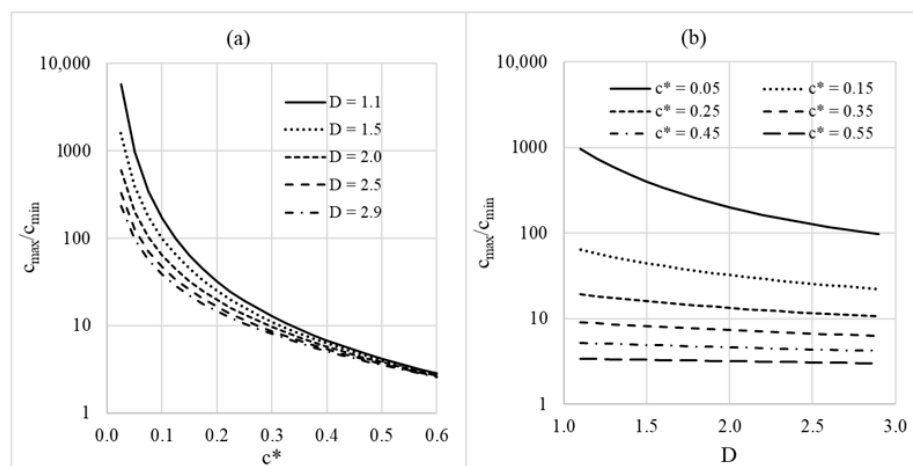


Figure 4. The influence of (a) mean particle concentration c^* and (b) fractal dimension D on the particle concentration range ratio c_{max}/c_{min} .

Figure 5 illustrates the impact of the fractal dimension on the mean superficial velocity ratio. For more dilute systems, the superficial velocity ratio is higher due to less hindered effects. While keeping the same mean particle concentration, the mean superficial velocity ratio decreases with the increasing fractal dimension. As the fractal dimension becomes larger for a given mean particle concentration, the two-phase system becomes more space-

filled and the range of concentration becomes smaller. The dilute regions that are mainly responsible for enhancing the superficial velocity are smaller when the fractal dimension becomes larger. As the superficial velocity decreases with the particle concentration quickly in a non-linear fashion, the mean superficial velocity also becomes smaller as the fractal dimension becomes larger.

Figure 6 shows the impact of the fractal dimension on the standard deviation of the superficial velocity ratio (Figure 6a) and on the standard deviation of the particle concentration (Figure 6b). The more space-filled system with the larger fractal dimension has smaller variability in the superficial velocity ratio. The standard deviation of the particle concentration itself also decreases with the increasing fractal dimension. For the particle concentration, when the mean concentration is smaller, its potential variability is also smaller. For the superficial velocity ratio, however, the higher variability corresponds to the condition of the lower mean particle concentration. When the mean particle concentration decreases, then both the mean and standard deviation of the superficial velocity ratio increase. It should be noted, however, that the coefficient of the variation of the superficial velocity ratio does not necessarily increase.

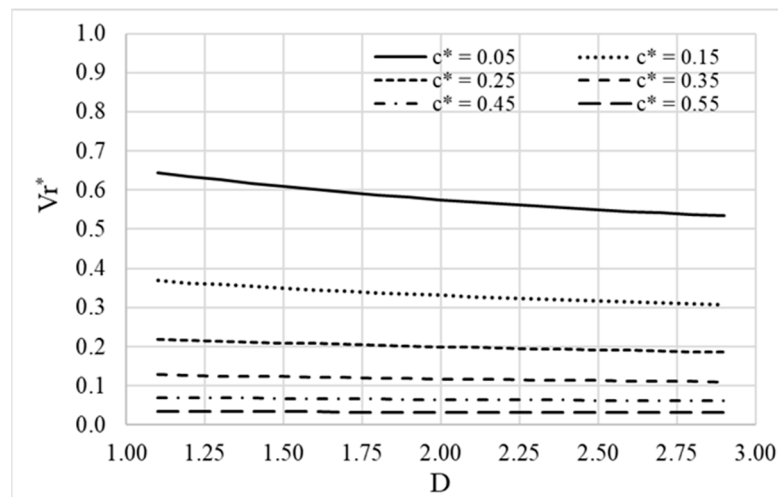


Figure 5. Impact of the fractal dimension D on the mean superficial velocity ratio V_r^* .

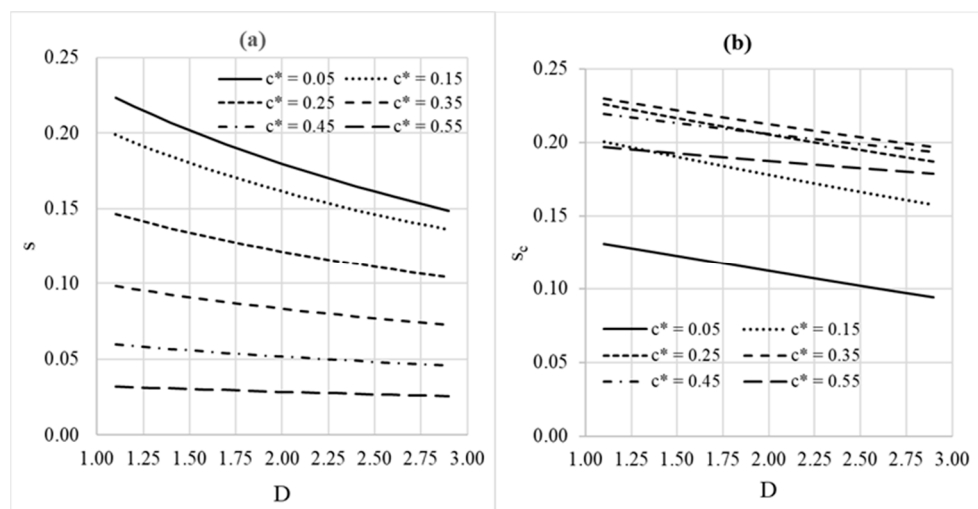


Figure 6. Impact of the fractal dimension D on the standard deviations of (a) the superficial velocity ratio s , and (b) the particle concentration s_c .

4. Discussion

While accurate superficial velocity relationships are of great practical importance, there is no definite consensus regarding the precise form on the superficial velocity. There have been many models to predict the superficial velocity in both sedimentation and fluidization, with most of them being empirical. One of the earliest empirical models by Richardson and Zaki [27] had the power-law form as $V_r = (1 - c)^{4.65}$. Most recently, Baas et al. [4] revised this equation by empirically formulating the constant power “4.65” in the Richardson and Zaki [27] as a decreasing function of the Reynolds number based on 548 data sets from the literature. In the slow flow regime, however, it was concluded that the power “4.65” was reasonable.

Hoef et al. [28] performed a Lattice-Boltzmann simulation of flow past arrays of spheres and fitted their results of drag force into an empirical formula, which can be translated into the superficial velocity ratio. More recently, Faroughi and Huber [29] proposed a theoretical model for the superficial velocity in the slow flow regime based on three sets of correction.

The model developed in this study is compared to these three models spanning over the last six decades from empirical, semi-empirical, and numerical studies, and the comparison results shown in Figure 7 include the mean superficial velocity ratios from the present study and those from Richardson and Zaki [27], Hoef et al. [28], and Faroughi and Huber [29] are plotted together for comparison. The models in the literature exhibited a wide range of variations. The early model of Richardson and Zaki [27] and the original free surface model [20] were the upper and lower bounds among the models compared in Figure 7. The present model integrating the truncated fractal distribution of particle concentration and those of Hoef et al. [28] and Faroughi and Huber [29] lie between these two models.

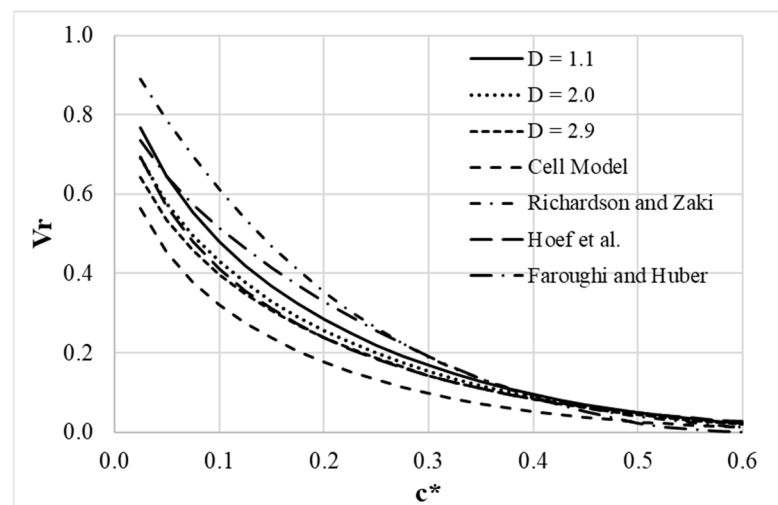


Figure 7. Comparison of the superficial velocity ratio from the present model with those from other representative models of Richardson and Zaki [27], Hoef et al. [28] and Faroughi and Huber [29] in the literature.

A unique relationship between the superficial velocity and particle concentration does not exist. The free surface cell model gives a lower bound and corresponds to the condition representing uniform particle distribution since any circulation or agglomeration effects result in an increased superficial velocity. In very dilute systems, particles are not close enough to attract each other, whereas in concentrated systems, mutual interference will result in a more or less uniform development of structure. The heterogeneity due to the agglomeration effects could be of greatest importance. In this study, we address spatially heterogeneous distribution in which the particle concentration in a portion of the regions is higher than the other locations. This type of spatial heterogeneity may also be indirectly generated by non-uniform particle size distribution, although the approach

proposed in this study does not directly address the particle size distribution and its effect on the superficial velocity of the two-phase system.

There are other factors that could potentially affect the superficial velocity such as the effects by column wall, particle shape, and cohesive forces, among others. The wall effects have been shown to decrease superficial velocity by friction at the column walls [30]. For most practical applications, however, the wall effect is considered negligible. Particle shape has been demonstrated to also impact the superficial velocity. Chong et al. [9], Chianese et al. [10], and Baldock et al. [31] showed that the superficial velocity was higher for spherical particles than for non-spherical particles due to the capture of stagnant fluid in the angularities of the non-spherical particles. Correction for particle shape usually requires laborious measurements of sphericity and the angularity of individual particles. Cohesive particles may also reduce the superficial velocity due to a magnified hindered effect by providing supportive strength [32,33].

The focus of this study is the impact of particle concentration heterogeneity on the superficial velocity of a two-phase system due to the factors such as particle aggregation and non-uniform particle size distribution. The heterogeneous particle concentration distribution is quantified by the fractal dimension D and the range reflected by the particle concentration ratio c_{\max}/c_{\min} . Other factors such as shape and its distribution may also be partially accounted for by the c_{\max}/c_{\min} range and D value, but its quantitative extent is difficult to assess and deserves further studies.

It should be noted that the approach computes the ensemble mean and the associated standard deviation of the superficial velocity ratio for the stationary two-phase heterogeneous system, in which the spatial mean can be represented by the ensemble mean. Based on the truncated fractal distribution of particle concentration, the superficial velocity ratio also has a random distribution. The approach does not, however, predict the explicit superficial velocity at each single region.

5. Conclusions

In this study, a new approach is developed to examine the impact of particle–fluid interaction on the superficial velocity in a heterogeneous multiparticle two-phase system. Locally, the interaction among particles and fluid is represented by the free surface cell model. The particle concentration is then assumed to follow a truncated fractal distribution. The main conclusions can be summarized as follows.

1. While the deterministic free surface cell model underestimates the superficial velocity, the free surface cell model that incorporates a truncated fractal distribution of particle concentration can predict a high superficial velocity ratio.
2. For a given mean particle concentration, a smaller fractal dimension means a higher ratio of maximum particle concentration over minimum particle concentration.
3. The mean superficial velocity ratio compares well with the experimental data in the literature, but the model still slightly underestimates the superficial velocity ratio in dilute two-phase systems.
4. For a two-phase system with a higher fractal dimension, both the mean superficial velocity ratio and the standard deviation of the superficial velocity ratio are smaller.

Funding: This research received no external funding.

Data Availability Statement: The data presented in this study are available on request from the corresponding author.

Conflicts of Interest: The author declares no conflict of interest.

References

1. Carey, V.P. Dependence of settling velocity on particle concentration in a fluidised bed of spherical particles. *Int. J. Multiph. Flow* **1987**, *13*, 429–431. [[CrossRef](#)]
2. Pal, D.; Ghoshal, K. Hindered settling with an apparent particle diameter concept. *Adv. Water Resour.* **2013**, *60*, 178–187. [[CrossRef](#)]
3. Pyles, D.R.; Straub, K.M.; Stammer, J.G. Spatial variations on the composition of turbidites due to hydrodynamic fractionation. *Geophys. Res. Lett.* **2013**, *40*, 3919–3923. [[CrossRef](#)]
4. Baas, J.H.; Baker, M.L.; Buffon, P.; Strachan, L.J.; Bostock, H.C.; Hodgson, D.; Eggenhuisen, J.T.; Spsychala, Y.T. Blood, lead and spheres: A hindered settling equation for sedimentologists based on metadata analysis. *Depos. Rec.* **2022**, *8*, 603–615. [[CrossRef](#)]
5. Lockett, M.J.; Al-Habbooby, H.M. Relative particle velocities in two-species settling. *Powder Technol.* **1974**, *10*, 67–71. [[CrossRef](#)]
6. Mirza, S.; Richardson, J.F. Sedimentation of suspensions of particles of two or more sizes. *Chem. Eng. Sci.* **1979**, *34*, 447–454. [[CrossRef](#)]
7. Scott, K.J.; Mandersloot, W.G.B. The mean particle size in hindered settling of multisized particles. *Powder Technol.* **1979**, *24*, 99–101. [[CrossRef](#)]
8. Felice, R.D. Hydrodynamics of liquid fluidization. *Chem. Eng. Sci.* **1995**, *50*, 1213–1245. [[CrossRef](#)]
9. Chong, Y.S.; Ratkowsky, D.A.; Epstein, N. Effect of particle shape on hindered settling in creeping flow. *Powder Technol.* **1979**, *23*, 55–66. [[CrossRef](#)]
10. Chianese, A.; Frances, C.; Di Berardino, F.; Bruno, L. On the behaviour of a liquid fluidized bed of monosized sodium perborate crystals. *Chem. Eng. J.* **1992**, *50*, 87–94. [[CrossRef](#)]
11. Ferguson, R.I.; Church, M. A simple universal equation for grain settling velocity. *J. Sediment. Res.* **2004**, *74*, 933–937. [[CrossRef](#)]
12. Camenen, B. Simple and general formula for the settling velocity of particles. *J. Hydraul. Eng.* **2007**, *133*, 229–233. [[CrossRef](#)]
13. Hanratty, T.J.; Bandukwala, A. Fluidization and sedimentation of spherical particles. *AIChE J.* **1957**, *3*, 293–296. [[CrossRef](#)]
14. Sun, Z.; Zhu, J. A four-quadrant flow regime map for two-phase liquid-solids and gas-solids fluidization systems. *Powder Technol.* **2021**, *394*, 424–438. [[CrossRef](#)]
15. Grace, J.R. Contacting modes and behaviour classification of gas-solid and other two-phase suspensions. *Can. J. Chem. Eng.* **1986**, *64*, 353–363. [[CrossRef](#)]
16. Liu, D.; Kwauk, M.; Li, H. Aggregative and particulate fluidization—The two extremes of a continuous spectrum. *Chem. Eng. Sci.* **1996**, *51*, 4045–4063. [[CrossRef](#)]
17. Sun, Z.; Zhu, J. A consolidated flow regime map of upward gas fluidization. *AIChE J.* **2019**, *65*, e16672. [[CrossRef](#)]
18. Felice, R.D.; Gibilaro, L.G.; Waldram, S.P.; Foscolo, P.U. Mixing and segregation in binary-solid liquid fluidised beds. *Chem. Eng. Sci.* **1987**, *42*, 639–652. [[CrossRef](#)]
19. Patwardhan, V.S.; Tien, C. Distribution of solid particles in liquid fluidized beds. *Can. J. Chem. Eng.* **1984**, *62*, 46–54. [[CrossRef](#)]
20. Happel, J. Viscous flow in multiparticle systems: Slow motion of fluids relative to beds of spherical particles. *AIChE J.* **1958**, *4*, 197–201. [[CrossRef](#)]
21. Jean, R.H.; Fan, L.-S. A fluid mechanic-based model for sedimentation and fluidization at low Reynolds numbers. *Chem. Eng. Sci.* **1989**, *44*, 353–362. [[CrossRef](#)]
22. Maude, A.D.; Whitmore, R.L. A generalized theory of sedimentation. *Br. J. Appl. Phys.* **1959**, *9*, 477–482. [[CrossRef](#)]
23. Zhu, J.; Satish, M.G. Non-Newtonian effects on the drag of creeping flow through packed beds. *Int. J. Multiph. Flow* **1992**, *18*, 765–777. [[CrossRef](#)]
24. Barua, D. A model-based analysis of tissue targeting efficacy of nanoparticles. *J. R. Soc. Interface* **2018**, *15*, 20170787. [[CrossRef](#)]
25. Mandelbrot, B.B. *The Fractal Geometry of Nature*; Macmillan: New York, NY, USA, 1983.
26. Miao, T.; Yu, B.; Duan, Y.; Fang, Q. A fractal analysis of permeability for fractured rocks. *Int. J. Heat Mass Transf.* **2015**, *81*, 75–80. [[CrossRef](#)]
27. Richardson, J.F.; Zaki, W.N. The sedimentation of a suspension of uniform spheres under conditions of viscous flow. *Chem. Eng. Sci.* **1954**, *8*, 65–73. [[CrossRef](#)]
28. Hoef, M.V.D.; Beetstra, R.; Kuipers, J.A.M. Lattice-Boltzmann simulations of low-Reynolds-number flow past mono- and bidisperse arrays of spheres: Results for the permeability and drag force. *J. Fluid Mech.* **2005**, *528*, 233–254. [[CrossRef](#)]
29. Faroughi, S.A.; Huber, C. Unifying the relative hindered velocity in suspensions and emulsions of nondeformable particles. *Geophys. Res. Lett.* **2015**, *42*, 53–59. [[CrossRef](#)]
30. Brea, F.M.; Edwards, M.F.; Wilkinson, W.L. The flow of non-Newtonian slurries through fixed and fluidised beds. *Chem. Eng. Sci.* **1976**, *31*, 329–336. [[CrossRef](#)]
31. Baldock, T.E.; Tomkins, M.R.; Nielsen, P.; Hughes, M.G. Settling velocity of sediments at high concentrations. *Coast. Eng.* **2004**, *51*, 91–100. [[CrossRef](#)]
32. Johnson, M.; Peakall, J.; Fairweather, M.; Biggs, S.; Harbottle, D.; Hunter, T.N. Characterization of multiple hindered settling regimes in aggregated mineral suspensions. *Ind. Eng. Chem. Res.* **2016**, *55*, 9983–9993. [[CrossRef](#)]
33. Spearman, J.; Manning, A.J. On the hindered settling of sand-mud suspensions. *Ocean. Dyn.* **2017**, *67*, 465–483. [[CrossRef](#)]